DARCY'S AND FORCHHEIMER'S LAWS IN PRACTICE. PART 2. THE NUMERICAL MODEL

Wojciech Sobieski[1], *Anna Trykozko*[2]

[1] Department of Mechanics and Machine Design
University of Warmia and Mazury in Olsztyn
[2] Interdisciplinary Centre for Mathematical and Computational Modeling
University of Warsaw

Abstract

Our study is based on a column experiment of water flow through a porous granular bed. In Part 1 we propose eight methods to derive parameters of flow models based on measurement data. These parameters are permeability and Forchheimer coefficient for Darcy's and Forchheimer's laws. The approach presented in this part uses two numerical models to perform simulations of flow. One model is based on the Finite Element Method implemented in the authors' code. The second model, which is ANSYS/Fluent package, uses the Finite Volume Method. Results of numerical computations are compared with experimental data that allows determination of the best method of parameter evaluation (in which the error was less than 3% over the whole range of filtration velocities). The problem of identification of ranges of applicability of the Darcy's and Forchheimer's laws is also addressed. In the conclusions, a set of guidelines is given, which should facilitate planning a similar experiment and its computational processing.

Introduction

In every experiment in which parameters are measured, and later used in a mathematical model, three main factors influence the quality of final results (SOBIESKI 2010b): precision of measuring equipment, a choice of a data processing method, and the accuracy of calculations. The current investigations are focused on the second aspect, in the context of modeling fluid flows through porous beds. Using different methods of data processing, we obtained several different values of permeability coefficient (Part 1). The aim of this

Correspondence: Wojciech Sobieski, Katedra Mechaniki i Podstaw Konstrukcji Maszyn, Uniwersytet Warmińsko-Mazurski, ul. M. Oczapowskiego 11, 10-957 Olsztyn, phone: +48 89 523 32 40, e-mail: wojciech.sobieski@uwm.edu.pl

paper is to apply numerical models in order to evaluate the quality of parameters. Numerical simulations reproducing the experiment were performed twice: based on the authors's code and applying the industry standard package ANSYS/Fluent (ANSYS Fluent 2014). Error analysis enabled the choice of the best method of data processing.

Numerical model of flow in porous media

The code we use solves the steady-state flow equation (BEAR 1972).

$$\nabla \cdot \left(\frac{\kappa}{\mu} \, \nabla p \right) = 0 \text{ in } \Omega \in R^3 \tag{1}$$

with
p – pressure [Pa],
κ – permeability [m^2],
μ – dynamic viscosity of the fluid [kg/(m·s)].

The permeability coefficient κ is a tensor in a general case (BREUGEM et al. 2004).

The domain Ω represents the column used in the experiments. Its boundary $\partial\Omega$ consists of three parts which are $\partial\Omega_{\text{wall}}$ – the side surface of the column, $\partial\Omega_{\text{out}}$ – the top of the column (outlet), and $\partial\Omega_{\text{in}}$ – the bottom of the column (inlet), $\partial\Omega = \partial\Omega_{\text{wall}} \cup \partial\Omega_{\text{out}} \cup \partial\Omega_{\text{in}}$.

The boundary conditions imposed on (1) are the following:

$$-\frac{\kappa}{\mu} \frac{\partial p}{\partial n} = 0 \text{ on } \partial\Omega_{\text{wall}} \text{ (no flow)} \tag{2a}$$

$$p = p_{\text{out}} \text{ on } \partial\Omega_{\text{out}} \tag{2b}$$

$$p = p_{\text{in}} \text{ on } \partial\Omega_{\text{in}} \tag{2c}$$

where p_{out} is a constant pressure on the outlet, p_{in} is a constant pressure on the inlet, both values are measured during the experiment.

Alternatively, one could replace (2c) with a condition imposing (a constant) flow rate v_{in} at the inlet, which is also available from the experiment:

$$-\frac{\kappa}{\mu}\frac{\partial p}{\partial n} = v_{in} \text{ on } \partial\Omega_{in} \tag{2d}$$

It is also possible to formulate equation (1) in terms of piezometric head h, $h = \frac{p}{\rho g} + z$, with denoting a fixed reference level, and conductivity coefficient **K** (Part 1, eq. 8). We assumed the reference level $z = 0$ is fixed at the bottom (inlet) of the pipe, thus the piezometric head at the outlet equals static pressure increased by the total length of the pipe. In particular, zero pressure at the outlet results in a piezometric head equal to the pipe's length.

Linear model

In order to solve (1) we applied Finite Element Method (FEM) (LUCQUIN, PIRONNEAU 1998) with linear basis functions constructed over tetrahedral elements. A cross-section of the computational domain is given in Figure 1. A mesh was created with the code Gambit (GAMBIT 2008), and then transformed to the format used by our code. As boundary conditions we used (2a), (2b), and (2d).

The system of linear equations was solved with a conjugate gradient method with a preconditioner based on incomplete Cholesky's decomposition (KAASSCHIETER 1988).
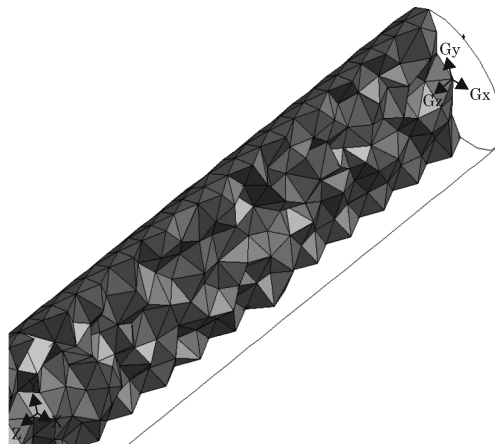

Fig. 1. Computational mesh – a cross-section

In a linear case filtration velocity $\vec{v}_f$ [m/s] can be obtained during a post-processing step using the Darcy's law:

$$\vec{v}_f = -\frac{\kappa}{\mu} \cdot \nabla p \qquad (3)$$

Solution of Eqn. (1) with homogeneous coefficients defined over a cylindrical geometry and with boundary conditions (2) is a linear function. Even if the case under study could be described as a one-dimensional problem we have decided to consider a full geometry of the experimental column.

Nonlinear model

It is possible to extend the code to model flows described by the nonlinear Forchheimer law by adding an outer iterative loop (FOURAR et al. 2005).

The algorithm is based on Forchheimer's law (Part 1, Eq. 5) rewritten in the form

$$\vec{v}_f^{(i+1)} = -\kappa_{\text{eff}}^{(i)} \cdot \nabla p \qquad (4)$$

where

$$\kappa_{\text{eff}}^{(i)} = \left(\frac{\mu}{\kappa} + \beta \cdot \rho \cdot |\vec{v}_f^{(i)}|\right)^{-1}, \quad i=1,... \qquad (5)$$

with the upper index (i) denoting an iteration number. Since $\kappa_{\text{eff}}^{(i)}$ depends on $\vec{v}_f^{(i)}$ which is not known *à priori*, we start the procedure assuming $\kappa_{\text{eff}}^{(0)} = \frac{\kappa}{\mu}$ and solving Eq. 1, which gives the first approximation of the velocity field $\vec{v}_f^{(1)}$ (Eq. 4). Iterations follow the scheme: new approximations of permeability coefficient $\kappa_{\text{eff}}^{(i)}$ (5) are computed elementwise. Eq. (1) is solved with updated permeabilities, providing a new approximation of velocity field (4).

As boundary conditions on $\partial\Omega_{\text{out}}$ and $\partial\Omega_{\text{in}}$ we impose (2b) and (2c) which are pressures measured during experiment.

Iterations are repeated until convergence is reached. The stopping criterion is evaluated at each iteration step by comparing a newly computed velocity field and velocities obtained in a former iteration. This iterative scheme is not computationally optimal, but offers an easy way to get solutions of a nonlinear model.

It would be possible to reformulate the algorithm in such a way that the inlet boundary condition is defined by (2d).

As observed in (GARIBOTTI, PESZYŃSKA 2009), such an iterative approach fails to converge for highly heterogeneous media, in our case however we deal with a homogeneous medium. The more general approach to solve the Forchheimer equation is to apply the nonlinear Newton solver (GARIBOTTI, PESZYŃSKA 2009).

Simulation model based on ANSYS/Fluent package

ANSYS/Fluent is a widely-used commercial package to numerically solve fluid dynamics problems described by universal balance equations. The standard system of mass balance (6) and momentum balance (7) of a fluid (AALTOSALMI 2005, Fluent Inc. 2006, SOBIESKI 2010a), supplemented with an appropriate source term is used:

$$\frac{\partial}{\partial t}\, \rho \,+\, \nabla(\rho \vec{v}) \,=\, 0 \tag{6}$$

$$\frac{\partial}{\partial t}\, (\rho \,\vec{v}) \,+\, \nabla(\rho \vec{v} \otimes \vec{v}) \,=\, \nabla(-\, p\ddot{I} \,+\, \ddot{\tau}\,) \,+\, \rho \vec{s_b} \tag{7}$$

where:
ρ – density of the fluid [kg/m^3],
$\vec{v}$ – velocity [m/s],
$\ddot{\tau}$ – total stress tensor [Pa],
$\vec{s_b}$ – source of mass forces [N/m^3],
p – static pressure [Pa],
I – unit tensor [–].

As one of its features Fluent offers modeling flows in porous media by the Porous Media Model (PMM) (SOBIESKI 2011, SOBIESKI 2013). In the PMM approach an additional flow resistance, taking a form of a source of mass forces, is added to the source term of momentum balance equation (7). This source may be described by Darcy's law, what corresponds to losses due to viscosity

$$s_{i,viscous} \,=\, -\sum_{j=1}^{3} D_{ij} \,\cdot\, \mu \,\cdot\, v_j \tag{8}$$

or by Forchheimer's law, taking into account losses due to viscosity and inertia

$$s_{i,interial} = - \sum_{j=1}^{3} D_{ij} \cdot \mu \cdot v_j - \sum_{j=1}^{3} D_{ij} \cdot \frac{\rho \cdot |v| \cdot v_j}{2} \tag{9}$$

or any other law defining flow through porous media (ANDRADE 1999, ANSYS Fluent 2014, PATIÑO 2003).

Notation used in (8)–(9) follows the notation used in Fluent documentation (Fluent Inc. 2006). Symbol s_i denotes source of forces for the i-th space dimension (x, y, and in a 3D case), μ – dynamic viscosity coefficient [kg/(m.s)], v_j – the j-th component of velocity [m/s], $|v|$ – absolute value of velocity [m/s]. **D** is a matrix with diagonal terms equal to l/κ, and **C** is a matrix with diagonal terms equal to 2β. Off-diagonal terms in both matrices are null. It is possible to take into account anisotropic flows in ANSYS/Fluent by means of additional parameters, but it is not discussed here.

State variables of the system (6)–(7): pressure p and velocity $\vec{v}$ are independent, whereas the flow equation (1) depends on p only, and velocity $\vec{v}$ is derived from (3). In this sense, the system (6)–(7) represents a more general description of the process.

Table 1

Specification of computer model parameters

Parameter	Value or description
Solver	pressure based, steady
Computation domain type	3D
Energy equation	switched off
Viscous Model	laminar
Fluid	water
Fluid density	994.49 [kg/m³]
Fluid viscosity	0.000743 [kg/(m · s)]
Operating pressure	101325 [Pa]
Gravitational acceleration	–9.81 [m/s²]
Inlet type	velocity inlet
Inlet water velocity	0.0003127 – 0.0100738 [m/s]
Outlet type	pressure outlet
Outlet air pressure	0.0 [Pa]

The PMM described by equations (6)–(7) together with the source term should not be confused with a microscopic representation of a porous medium, where flow occurs in 'empty' void space (pores) of a medium and which is described by a set of Navier-Stokes' equations (as for instance in (PESZYŃSKA, TRYKOZKO 2013, VAKILHA, MANZARI 2008)). At a macroscopic scale these channels are not visible and averaged values are used instead. This is the case in the PMM applied in Fluent, which uses a source term in order to get averaged flow.

The geometry of the domain as well as the computational mesh were created with the Gambit package. Values of parameters used in Fluent are collected in Table 1.

Results and discussion

Simulations presented in this section were performed with the two codes described in sections 2 and 3. As parameters of the computational models we used experimentally-obtained parameters computed with all the methods proposed in Part 1, Sections 3 and 4.

Figure 1 gives the results of simulations obtained with the linear model and four different values of permeability computed with the four methods (Part 1, Sec. 3). We assumed that only four experiments (2–5) belong to the ranges of Darcy's law validity. A similar summary was performed for the nonlinear model with parameters described in Part 1, Sec. 4 (Fig. 2). In this case all filtration velocities $\vec{v}_f$ used in the experiment were taken into account. Numbers on plots denote measurement numbers and refer to Table 2 in Part 1. Results presented in Figs. 1 and 2 were obtained with the ANSYS/Fluent code.

Figures 1 and 2 allow comparison between static pressures obtained numerically and experimentally in measurement points along the column. In order to study the character of changes in pressure values between the extreme measurements points in function of filtration velocity, additional plots were made (Figs. 3 and 4), which will be referred to as flow characteristics. Figures 3 and 4 contain computational results obtained with the two codes. Since numerical results are identical, in further analysis and computations only results obtained with the ANSYS/Fluent code are considered. Software written by the authors was used to postprocess ANSYS/Fluent results, thus automating and significantly accelerating a single computation cycle.
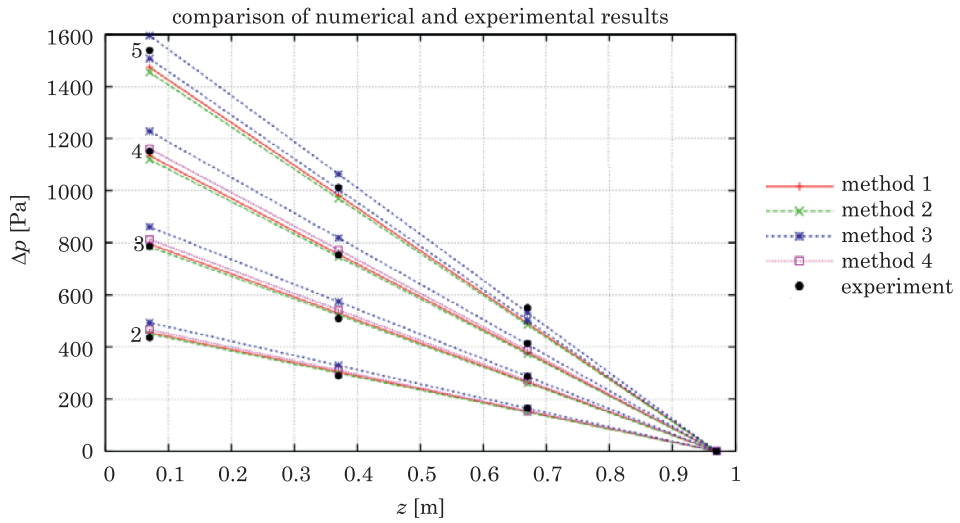
Fig. 1. Distribution of pressure along the column as a function of filtration velocity obtained by numerical simulations of linear model (continuous lines) and in measurements (points)
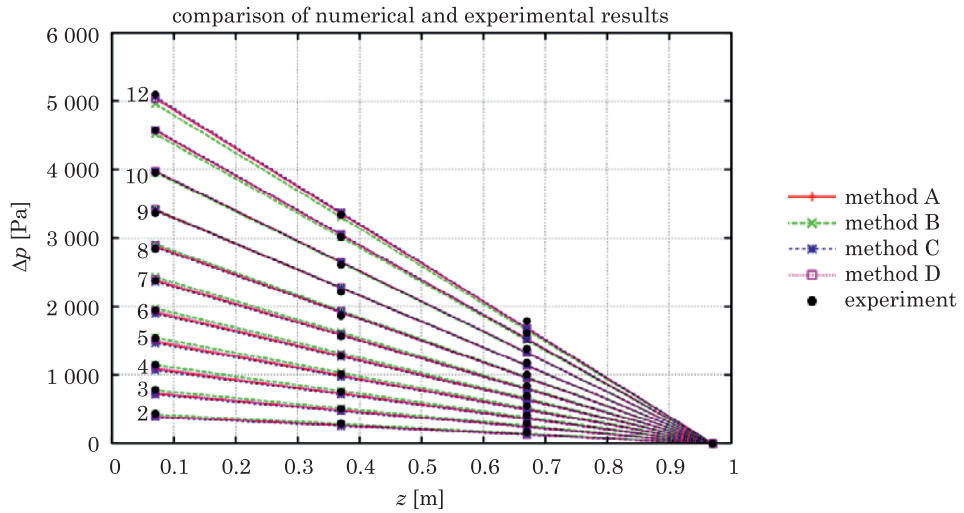

Fig. 2. Distribution of static pressure along the column axis as a function of filtration velocity obtained by numerical simulations of nonlinear model (continuous lines) and in measurements (points)

comparison of numerical and experimental results — linear model

Fig. 3. Comparison of pressure drop as a function of velocity obtained numerically and experimentally for a linear model

comparison of numerical and experimental results — nonlinear model
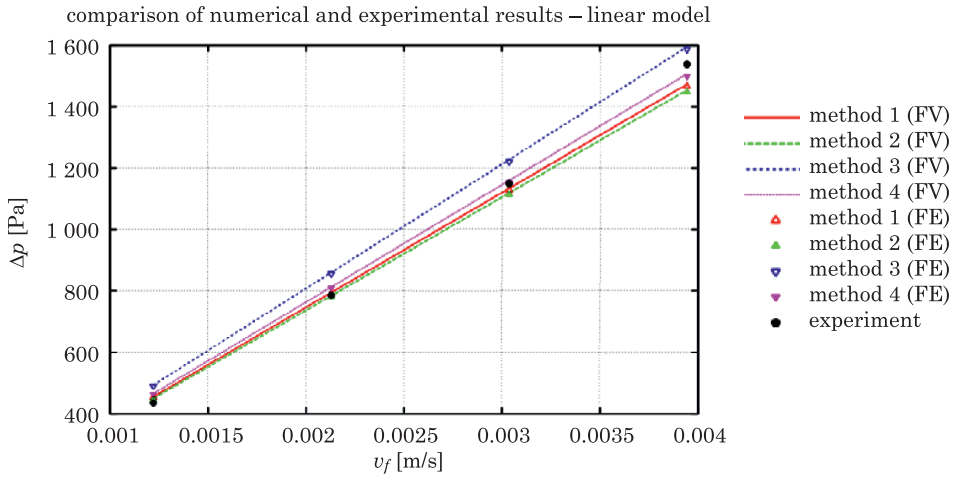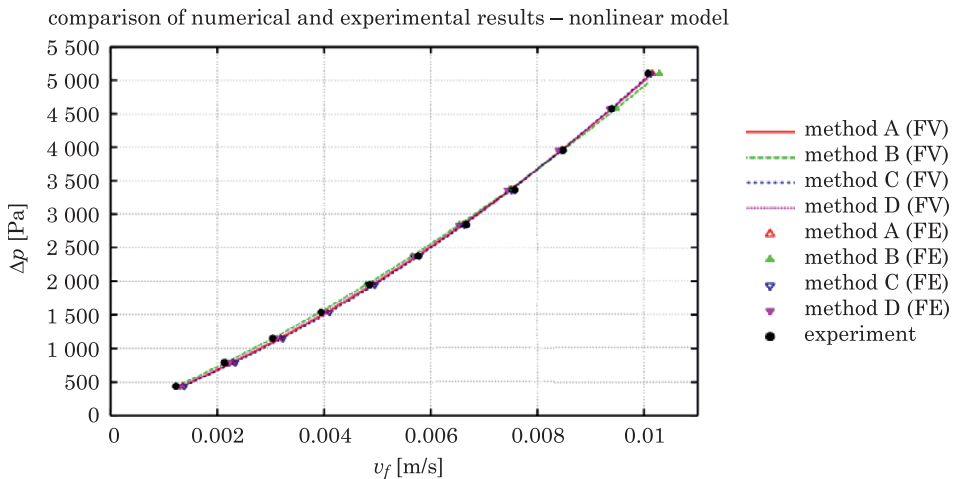

Fig. 4. Comparison of pressure drop as a function of velocity obtained numerically and experimentally for a nonlinear model

Error analysis

In order to find which of the methods used to compute model parameters provides the best agreement with measurements, an error analysis was performed. The percentage error δ_{i-0} was computed from the formula:

$$\delta_{i-0} = \left| \frac{x_i - x_0}{x_0} \right| \cdot 100\% \tag{10}$$

where:

x_i – numerically computed value of a state variable,

x_0 – the exact value (obtained experimentally).

Only directly measured values (as opposed to values obtained with approximation methods) were taken as x_0. Results for the four linear models (denoted with upper indexes) are given in Tables 2–4.

For the linear model, the error, reaching several percent, appeared for method 3 of permeability computation. Moreover, the flow characteristic is shifted upwards with respect to the measurement data, and all errors were of positive values. All remaining simulations, based on methods 1, 2, and 4, give similar results. Errors are smaller and of different signs. This error analysis shows that averaging methods perform better. Method 2 based on measurements at all measurements points along the column seems to be more relevant than method 1, or method 4, which is restricted to extreme measurement points.

Table 2

Percentage errors for a segment between measurement points 4 and 1

$\vec{v}_f$	$\Delta p_{4-1}^{\exp}$	Δp_{4-1}^1	Δp_{4-1}^2	Δp_{4-1}^3	Δp_{4-1}^4	δ_{4-1}^1	δ_{4-1}^2	δ_{4-1}^3	δ_{4-1}^4
$\cdot 10^{-3}$ [m/s]	[Pa]	[Pa]	[Pa]	[Pa]	[Pa]	[%]	[%]	[%]	[%]
1.2207	436.09	455.90	450.04	493.54	466.36	4.54	3.20	13.17	6.94
2.1287	786.33	795.03	784.80	860.67	813.25	1.11	–0.19	9.45	3.42
3.0367	1150.22	1134.15	1119.56	1227.78	1160.15	–1.40	–2.66	6.74	0.86
3.9447	1538.51	1473.28	1454.32	1594.90	1507.05	–4.24	–5.47	3.66	–2.04

Table 3

Percentage errors for a segment between measurement points 3 and 1

$\vec{v}_f$	$\Delta p_{3-1}^{\exp}$	Δp_{3-1}^1	Δp_{3-1}^2	Δp_{3-1}^3	Δp_{3-1}^4	δ_{3-1}^1	δ_{3-1}^2	δ_{3-1}^3	δ_{3-1}^4
$\cdot 10^{-3}$ [m/s]	[Pa]	[Pa]	[Pa]	[Pa]	[Pa]	[%]	[%]	[%]	[%]
1.2207	288.78	303.94	300.03	329.03	310.90	5.25	3.89	13.94	7.66
2.1287	509.26	530.02	523.20	573.78	542.17	4.08	2.74	12.67	6.46
3.0367	753.16	756.10	746.37	818.52	773.43	0.39	–0.90	8.68	2.69
3.9447	1012.67	982.18	969.55	1063.27	1004.70	–3.01	–4.26	4.10	–0.79

Table 4

Percentage errors for a segment between measurement points 2 and 1

$\vec{v}_f$	$\Delta p_{2-1}^{\exp}$	Δp_{2-1}^1	Δp_{2-1}^2	Δp_{2-1}^3	Δp_{2-1}^4	δ_{2-1}^1	δ_{2-1}^2	δ_{2-1}^3	δ_{2-1}^4
$\cdot\, 10^{-3}$ [m/s]	[Pa]	[Pa]	[Pa]	[Pa]	[Pa]	[%]	[%]	[%]	[%]
1.2207	164.88	151.97	150.01	164.51	155.45	–7.83	–9.02	–0.22	–5.72
2.1287	286.82	265.01	261.60	286.89	271.08	–7.60	–8.79	0.02	–5.49
3.0367	413.65	378.05	373.19	409.26	386.72	–8.61	–9.78	–1.06	–6.51
3.9447	550.23	491.09	484.77	531.63	502.35	–10.75	–11.90	–3.38	–8.70

As a next conclusion we get a confirmation of the assumption that the pressure drop should be computed based on the extreme measurement points. Using shorter segments between measurement points increases error values and results in a poorer quality of flow characteristics. This effect was already mentioned while discussing the influence of measurement point choice on the value of the permeability coefficient. A sequence of numerical simulations was performed (not described in this paper), with permeability coefficient computed based on pressure differences between measurement points 1–3, 2–4, and 2–3. The largest errors were encountered for the 2–3 case.

A visible difference of slopes of characteristics obtained for experiment and simulations is observed for the linear models (Fig. 3). This feature seems to be independent of the method of determining the permeability coefficient and may manifest the influence of other factors. It is possible that, in spite of relatively small Reynolds numbers, an influence of inertial losses is pronounced in our data (the same conclusion was stated in Part 1). This creates difficulty in defining the upper limit of Darcy's law validity with our results. Given our range of Re, this is consistent with the literature.

A similar error analysis performed for the nonlinear model indicates that method B provides the best values of coefficients for the Forchheimer equation. For the section between measurement points 4 and 1 (Table 5), errors for this method did not exceed 3%, which is a very good result. For the remaining methods, the errors were larger, in particular for smaller values of filtration velocity. Another indication in favor of method B is obtained by comparing averaged values of the absolute percentage error, which were for methods A, B, C, and D equal to 3.04, 1.57, 3.67 and 45%, respectively. As in the linear case, percentage errors were additionally computed taking into account shorter measurement segments. Again, a visible increase of errors followed a reduction the measurement segment length. Therefore measurements aimed at getting coefficients of nonlinear model should be conducted for the widest possible (available) range of filtration velocities, in spite of the range appropriate for the actual context of study.

Table 5

Percentage errors for computations based on nonlinear model

$\vec{v_f}$	$\Delta p_{4-1}^{\exp}$	Δp_{4-1}^{A}	Δp_{4-1}^{B}	Δp_{4-1}^{C}	Δp_{4-1}^{D}	δ_{4-1}^{A}	δ_{4-1}^{B}	δ_{4-1}^{C}	δ_{4-1}^{D}
$\cdot 10^{-3}$ [m/s]	[Pa]	[Pa]	[Pa]	[Pa]	[Pa]	[%]	[%]	[%]	[%]
1.2207	436.09	391.38	424.97	382.57	401.74	–10.25	–2.55	–12.27	–7.88
2.1287	786.33	721.81	772.60	708.46	737.89	–8.20	–1.75	–9.90	–6.16
3.0367	1150.22	1085.78	1147.10	1069.60	1105.87	–5.60	–0.27	–7.01	–3.86
3.9447	1538.51	1483.27	1548.50	1466.01	1505.68	–3.59	0.65	–4.71	–2.13
4.8527	1946.31	1914.32	1976.77	1897.66	1937.33	–1.64	1.56	–2.50	–0.46
5.7608	2378.50	2378.92	2431.98	2364.62	2400.87	0.02	2.25	–0.58	0.94
6.6688	2842.88	2877.04	2914.02	2866.79	2896.18	1.20	2.50	0.84	1.87
7.5768	3366.77	3408.67	3422.95	3404.21	3423.33	1.24	1.67	1.11	1.68
8.4848	3956.03	3973.85	3958.76	3976.89	3982.33	0.45	0.07	0.53	0.66
9.3928	4576.51	4572.55	4521.45	4584.81	4573.15	–0.09	–1.20	0.18	–0.07
10.0738	5101.38	5043.58	4961.11	5063.89	5037.15	–1.13	–2.75	–0.73	–1.26

Error analysis resulted in new data for a discussion on the limits of Darcy's and Forchheimer laws validity. Small errors encountered for the model B indicate that it is the most appropriate model to describe the flow within the whole velocity range.

Summary and conclusions

As a result of our studies a number of conclusions can be formulated:

– Forchheimer's law (with parameters computed with the Forchheimer Plot Method) gives better results for the whole range of flow velocities. For small Reynolds numbers, the contribution of the nonlinear term is small and the model becomes quasi-linear. Application of Forchheimer's law allows to avoid the error in estimating the flow regime – and the true character of flow is automatically manifested in simulations (provided a series of computations for a range of filtration velocities is performed).

– In spite of the latter statement, there exists a range of filtration velocities where linear models are an appropriate approximation and may be successfully applied. It is extremely important, because of a relative simplicity of linear models.

Our results suggest that for a wider range of different flow velocities relying only on Reynolds numbers and related literature-based upper bounds for Darcy's law validity may prove insufficient.

– To ensure a good quality of parameters, it is important to conduct as many measurements as possible for different filtration velocities. A single measurement (or a series but with the same parameters) may prove insufficient. Also, the larger range of filtration velocities is used in measurements, the more exact derived parameters are.

– Pressure drop should be defined based on measurements over the longest possible segment, fitted to a kind of a medium under study and a size of available samples. Taking shorter segments resulted in larger errors.

– Once parameters of a medium are known, simulating flow through a typical porous medium poses no problem. Several methods of computing permeability as well as Forchheimer coefficient were presented.

– It is essential to carefully measure piezometric heads (or pressures) in measurement points. Permeability coefficient is computed on their basis and the model is very sensitive to this parameter.

– Software used to model porous media may be based on a flow equation or on more general formulations of balance equations. A particular choice of a numerical method to solve equations (Finite Volume Method, Finite Element Method) seems not to have too much influence.

References

AALTOSALMI U. 2005. *Fluid Flow in Porous Media with the Lattice-Boltzmann Method*. PhD Thesis. Department of Physics, University of Jyväskylä. Finland, July.

ANDRADE J.S., COSTA U.M.S., ALMEIDA M.P., MAKSE H.A., STANLEY H.E. 1999. *Inertial Effects on Fluid Flow through Disordered Porous Media*. Physical Review Letters, 82(26), 5249–5252.

BEAR J. 1972. *Dynamics of Fluids in Porous Media*. Dover, New York.

BREUGEM W.P., BOERSMA B.J., UTTENBOGAARD R.E. 2004. *Direct numerical simulations of plane channel flow over a 3D Cartesian grid of cubes*. In: *Applications of porous media (ICAPM 2004)*. Eds. A.H. Reis, A.F. Miguel. Evora Geophysics Center,. Évora, pp. 27–35.

ANSYS Fluent Home Page. 2014. On line:: http://www.ansys.com/Products/Simulation+Technology/Fluid+Dynamics/Fluid+Dynamics+Products/ANSYS+Fluent (access: 1 April 2014).

Fluent Inc. 2006. Fluent 6.3 User's Guide (September 2006), Chapter 7.19: Porous Media Conditions.

FOURAR M., LENORMAND R., KARIMI-FARD M. 2005. *Inertia Effects in High-Rate Flow Through Heterogeneous Porous Media*. Transport in Porous Media, 60(3): 353–370.

GAMBIT Home Page 2008. On line: http://www.fluent.com/software/gambit/index.htm (access: 1 March 2008).

GARIBOTTI C., PESZYŃSKA M. 2009. *Upscaling non-Darcy flow*. Transport in Porous Media, 80(3): 401–430.

KAASSCHIETER E.F. 1988. *Preconditioned conjugate gradients for solving singular systems*. Journal of Computational and Applied Mathematics, 24(1–2): 265–275.

LUCQUIN B., PIRONNEAU O. 1998. *Introduction to Scientific Computing*. Wiley. Chichester.

PATIÑO O.A.L. 2003. *Optimisation of Heat Sinks by Computational Flow Dynamics Techniques*. PhD Thesis. Gent University, Gent, Belgium.

PESZYŃSKA M., TRYKOZKO A. 2013 *Pore-to-core simulations of flow with large velocities using continuum models and imaging data*. Computational Geosciences, 17(4): 623–645.

SOBIESKI W. 2010a. *Examples of Using the Finite Volume Method for Modeling Fluid-Solid Systems*. Technical Sciences, 13: 256–265.

SOBIESKI W. 2010b. *Use of Numerical Models in Validating Experimental Results*. Journal of Applied Computer Science, 18(1): 49–60.

SOBIESKI W. 2011. *The Basic Equations of Fluid Mechanics in Form Characteristic of the Finite Volume Method*. Technical Sciences, 14(2): 299–313.

SOBIESKI W. 2013. *The Basic Closures of Fluid Mechanics in Form Characteristic for the Finite Volume Method*. Technical Sciences, 16(2): 93–107.

VAKILHA M., MANZARI M.T. 2008. *Modelling of Power-law Fluid Flow Through Porous Media Using Smoothed Particle Hydrodynamics*. Transport in Porous Media, 74(3): 331–346.